Full-Azimuth Angle Domain Imaging

Zvi Koren, Igor Ravve, Evgeny Ragoza, Allon Bartana, Paradigm Geophysical,
Dan Kosloff, Tel Aviv University and Paradigm Geophysical

Summary
This work presents a new seismic imaging system for generating and extracting high-resolution information about subsurface angle dependent reflectivity, with simultaneous emphasis on both continuous structural surfaces and discontinuous objects, such as faults and small-scale fractures. The system enables full-azimuth, angle-dependent seismic imaging using reflection data recorded through seismic acquisition surveys, especially wide-azimuth and long offset data. Geometrical attributes, such as dip-azimuth and continuity of the local reflecting surfaces, can be automatically extracted directly from the full-azimuth angle gathers. Azimuthal anisotropy can be detected, leading to an accurate anisotropy model representation.

Introduction
The theory and implementation of imaging methods in the Local Angle Domain (LAD) have been intensively studied (e.g., Miller et al., 1987, de Hoop and Bleistein, 1997, Brandsberg-Dahl et al. 1999, Rousseu et al. 2000, Xu et al., 2001, Audebert et al. 2002, Biondi and Symes, 2004, Ursin, 2004, Wu et al. 2006, Biondi, 2007).

The imaging engine of the proposed system is an extension of the Common Reflection Angle Migration (CRAM), (Koren et al., 2002). CRAM is a multi-arrival, ray-based migration that uses the whole wavefield within a controlled aperture. Unlike conventional ray-based imaging methods, the ray tracing is performed from image points (in all directions, including turning rays) up to the surface, forming a system for mapping the recorded surface seismic data into the Local Angle Domain (LAD) at the image points (Koren et al, 2007). The procedure is based on a uniform illumination at the image points from all directions, ensuring that all arrivals are taken into account while amplitudes and phases are preserved.

CRAM is specifically designed for a number of seismic imaging and analysis tasks: Detailed velocity model determination; target-oriented, high-resolution reservoir imaging; accurate AVA and reservoir property extraction; and imaging data recorded in areas of complex structure and velocity. The migration supports isotropic and anisotropic models, and can be performed using all types of marine and land datasets, including OBC/OBS.

The CRAM migration is extremely versatile. It can be performed for full-volume and full-aperture imaging, using clusters with a massive amount of nodes. It can also be run over specific small areas of interest with background dip-azimuth information, leading to a model-driven aperture, providing relatively fast and extremely high-quality and high-resolution performance.

The proposed extension, referred to here as Wide Eye CRAM, generates new, full-azimuth, angle domain common image gathers. In this abstract, we present the method and applications for the new angle gathers within the seismic exploration workflow

The Method
The proposed method follows the concept of working in the Local Angle Domain (LAD) in isotropy/anisotropy subsurface models. The asymptotic migration/inversion operator (ray paths, traveltimes, geometrical spreading and phase rotation factors) are calculated from the image points up to the surface, forming a system for mapping the recorded surface seismic data into the LAD at the image points. The strength of the proposed Wide Eye CRAM system is mainly its ability to construct different types of high-quality Angle Domain Common Image Gathers (ADCIG), representing full-azimuth angle dependent reflectivity in real 3D space. First, we create directional image gathers, containing both specular and scattered (diffraction) energy. The ability to decompose the principal direction of the specular energy from the total scattered (diffraction) field enables the extraction of geometrical subsurface attributes (e.g., dip-azimuth and continuity) directly from the (pre-stack) directional image gathers. The energy computed along the angle gather values is used as a weighted stack filter. Two types of images are then constructed: A specular weighted stack for emphasizing subsurface structure continuity, and a diffraction weighted stack, emphasizing small-scale objects like faults, channels and fractures. Specular weighted full-azimuth reflection angle image gathers are then created by integrating all of the seismic data points reflected/diffracted from the image points with the same opening (reflection/diffraction) angle and the same rotating azimuth angle. Due to the uniform illumination (mapping) in the angle domain, all arrivals are taken into account, thus obtaining continuous amplitude and phase preserved image gathers for a wide range of angles. Full-azimuth angle domain residual moveouts are automatically detected to update the background anisotropy model. These types of full-azimuth subsurface ADCIGs, especially when created in the area of the reservoir, open a new field for the determination of petrophysical parameters from seismic data.

Local Angle Domain: Ray Angles at Reflection Point

Imaging systems involve the interaction of two wavefields at the image points (elements): Incident and reflected/ diffracted. Each wavefield can be decomposed into local plane waves (or rays), indicating the direction of propagation. The direction of the incident and scattered rays can be conventionally described by their respective polar angles. Each polar angle includes two components - dip and azimuth. Therefore, a set of four scalar angles is required to define an angle domain imaging system at a given image point. Ray-based and wave-equation angle-domain migrations deal with angle systems in which both the incident and reflected wavefields at each image point are composed of a wide range of directions. The imaging stage involves combining a huge number of ray pairs (or pairs of local plane waves) representing the incident and reflected/diffracted rays. Each ray pair maps seismic data recorded on the free surface, into the four-dimensional Local Angle Domain (LAD) space (Koren et al., 2007). In our notation, these angles are dip ν_1 and azimuth ν_2 of the ray-pair normal, half opening angle γ_1 and opening azimuth γ_2. We establish relationships between the directions of the ray pairs and the LAD angles. Figure 1 shows an example of a selected ray pair (incident and scattered) and the four angles associated with the LAD. The LAD system may be associated with an axial cross-section of a conic surface. The axis of the cone coincides with the ray pair normal, i.e., it has the same orientation (dip and azimuth). The opening of the cone matches the opening angle, and the orientation of the cross-section corresponds to the opening azimuth.

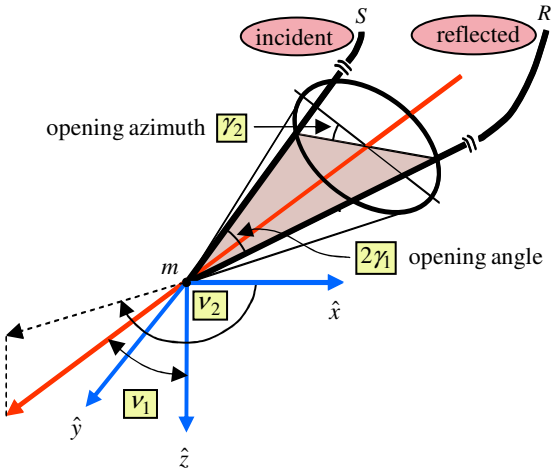

Figure 1. An example of a selected ray pair (incident and scattered) and the four angles associated with the LAD.

Migration Formula

Two types of angle domain common-image gathers (ADCIG) are created: directional and reflection. In the directional subsystem, the reflectivity I at the image point is a function of the ray pair normal zenith ν_1 and azimuth ν_2,

$$I_\nu(m,\nu_1,\nu_2)=\frac{\cos^2\nu_1}{V^2(m)}\int\frac{D_3(S,R,\tau_D)}{A(m,S)A(m,R)}\sin\gamma_1\,d\gamma_1 d\gamma_2 \quad . \quad (1)$$

In the reflection subsystem, the reflectivity I at the image point is a function of the opening angle γ_1 and the opening azimuth γ_2,

$$I_\gamma(m,\gamma_1,\gamma_2)=\frac{\cos^2\gamma_1}{V^2(m)}\int\frac{D_3(S,R,\tau_D)}{A(m,S)A(m,R)}\sin\nu_1\,d\nu_1 d\nu_2 \quad , \quad (2)$$

where

$$S=S(m,\nu_1,\nu_2,\gamma_1,\gamma_2)\ , \qquad R=R(m,\nu_1,\nu_2,\gamma_1,\gamma_2) \qquad (3)$$

are the shot and receiver coordinates on the surface. These coordinates are established by ray tracing that starts at a given image point, with initial ray parameters (phase velocities) that correspond to a given set of LAD angles (output-driven approach). Parameters

$$A(m,S)=\sqrt{\frac{V(m)}{8\pi\left|J(m,S)\right|}}\ , \quad A(m,R)=\sqrt{\frac{V(m)}{8\pi\left|J(m,R)\right|}} \qquad (4)$$

are Green's functions,

$$D_3[S,R,\tau_D(m,S,R)]=\int i\,w\,U(S,R,w)\,e^{i\Phi_3}\,dw \qquad (5)$$

is the filtered data,

$$\Phi_3=-w\,\tau_D(m,S,R)+\frac{\pi}{2}K(m,S,R)\,\mathrm{sgn}(w) \qquad (6)$$

is the phase, $U(S,R,w)$ is the input seismic trace, $K(m,S,R)$ is the KMAH index, $\tau_D=\tau_D(S,m,R)$ is the diffraction stack time. $V(m)$ is a function of the medium parameters; in the case of an isotropic model it coincides with the velocity. Lastly, J is the geometrical spreading. Equations 1 and 2 describe an output-driven approach, where the input seismic data to be migrated become functions of the LAD angles at the image points. Thus, theoretically, every ray pair used in the migration requires access to a different seismic trace. The random access to the input data makes it very difficult to implement this type of process. In addition, this approach requires a huge amount of memory for storing the input data.

Full-Azimuth Angle Domain Common Image Gathers

Figure 2 presents an example of displays of the full-azimuth angle domain common image gathers. The left upper plot shows a depth migrated section from 3D land data. The vertical line shows the lateral (in-line – cross-line) location of a specific gather, with a specific image point in depth marked on this line. A reflection angle gather

at this location, in a given azimuth, is shown in the left lower image. The right upper corner shows two spherical displays related to the specific image point. The right sphere represents the specular and diffused energy as a function of the dip/azimuth direction. The location of the spot on the sphere indicates that the image point is located in the vicinity of an actual reflecting surface. The orientation of the local reflecting surface is defined by the dip/azimuth indicated by the maximum energy value. For a real reflector, the size of the spot on the directional image is normally a relatively small area in the proximity of the specular direction. The specular component is attenuated relative to the scattered component (Kozlov et al., 2004). The left sphere represents the reflectivity vs. the opening angle and opening azimuth. For a real reflector, the opening angle range on the reflection image is normally large and is limited by the data acquisition. The right lower plot is a cylindrical display related to all vertical points of the gather. These points have a fixed lateral location and different depths. The cylindrical display includes a number of disks, where each disk is related to a specific point. The disk image is obtained from the spherical image by projecting or expanding the spherical surface on a planar surface.

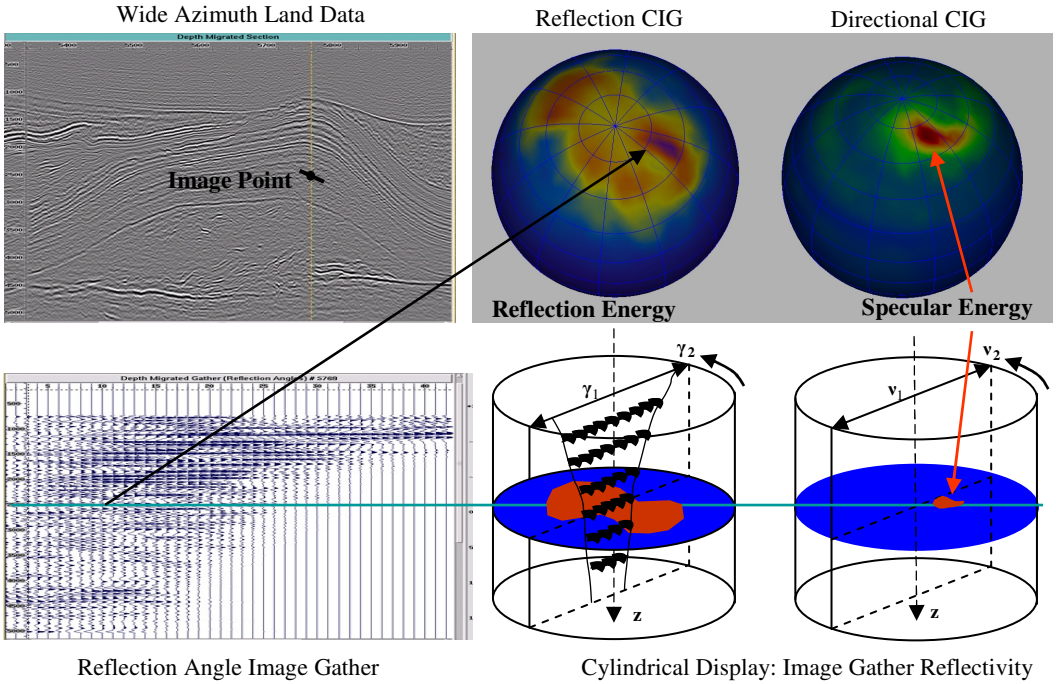

Figure 2. Angle domain reflectivity at image point

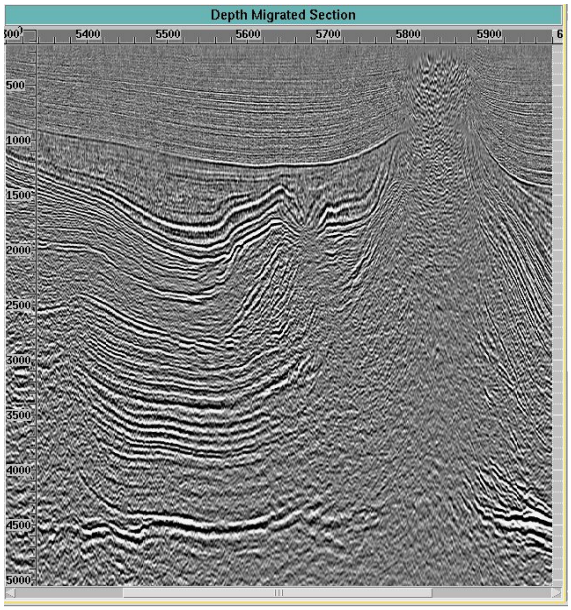

Figure 3a. CRAM 3D – Final image

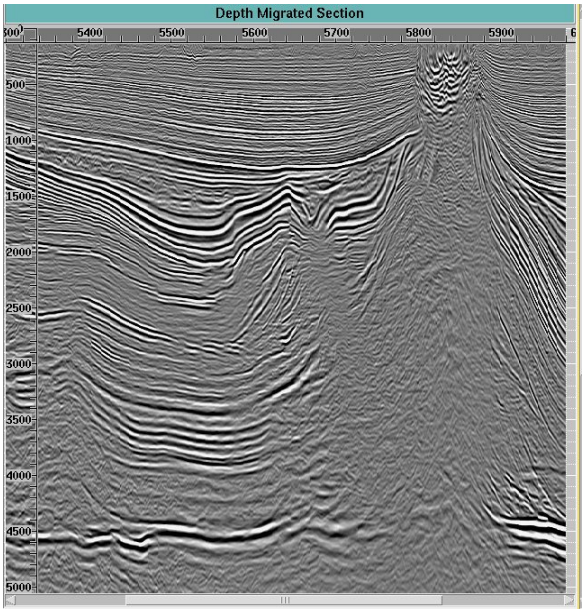

Figure 3b. Wide Eye CRAM 3D specular weighted stack

Field Example

Figure 3a shows a depth migrated section from 3D land data in Northwest Germany (owned by RWE-DEA AG and Wintershall AG). The depth image was created by stacking the traces within the reflection angle gathers generated by CRAM 3D (Equation 2). Although the image is relatively noisy, it contains the important details of the structure. Figure 3b shows the same line, where the depth image was created using Wide Eye CRAM. In this case, the energy values computed from the full-azimuth directional angle gathers are used as weighting factors in the total summation. The high "energy" values associated with the specular directions sharpen the image of the structure, while the diffusion (scattered) energy removes the internal noise, resulting in a much clearer image.

Conclusions

This work presents a novel imaging system for generating continuous, full-azimuth angle domain images. The system enables the automatic extraction of high-resolution information about the subsurface model. Both continuous structure surfaces and sub-scale small objects, such as channels and fractures, can be detected, even below complex geological structures. The new directional image gathers provide the automatic extraction of geometrical attributes, such as dip-azimuth and continuity. The new reflection angle gathers provide information about full-azimuth residual moveouts and amplitude variations, for direct indication of azimuthal anisotropy and fractures. It is a target-oriented system, providing direct, high-resolution reservoir imaging, and high-resolution information in the vicinity of wells.

Acknowledgments

We would like to thank RWE-DEA AG and Wintershall AG for their permission to use their data in this study. We would also like to thank Paradigm for its support and for permission to publish this paper.

EDITED REFERENCES

Note: This reference list is a copy-edited version of the reference list submitted by the author. Reference lists for the 2008 SEG Technical Program Expanded Abstracts have been copy edited so that references provided with the online metadata for each paper will achieve a high degree of linking to cited sources that appear on the Web.

REFERENCES

Audebert, F., P. Froidevaux, H. Rakotoarisoa, and J. Svay-Lucas, 2002, Presented at the 72nd Annual International Meeting, SEG.

Biondi, B., 2007, Residual moveout in anisotropic angle-domain common-image gathers: Geophysics, **72**, S93–S103.

Biondi, B., and W. Symes, 2004, Angle-domain common-image gathers for migration velocity analysis by wavefield-continuation imaging, Geophysics, **69**, 1283–1298.

Bleistein, N., Y. Zhang, S. Xu, G. Zhang, and S. H. Gray, 2005, Kirchhoff inversion in image point coordinates recast as source/receiver point processing: 75th Annual International Meeting, SEG, Expanded Abstracts, 1697–1700.

Brandsberg-Dahl, S., M. V. de Hoop, and B. Ursin, 1999, Velocity analysis in the common scattering-angle/azimuth domain: 69th Annual International Meeting, SEG, Expanded Abstracts, 1715–1718.

de Hoop, M. V., and N. Bleistein, 1997, Generalized radon transform inversions for reflectivity in anisotropic elastic media: Inverse Problems, **13**, 669–690.

Koren, Z., I. Ravve, A. Bartana, and D. Kosloff, 2007, Local angle domain in seismic imaging: Presented at the 69th Annual International Conference and Exhibition.

Koren, Z., X. Sheng, and D. Kosloff, 2002, Target-oriented common-reflection angle migration: Presented at the 72nd Annual International Meeting, SEG, Expanded Abstracts.

Kozlov, E., N. Barasky, and E. Korolev, 2004, Imaging scattering objects masked by specular reflections.

Miller, D., M. Oristaglio, and G. Beylkyn, 1987, A new slant on seismic imaging: Migration and integral geometry: Geophysics, **52**, 943–964.

Rosseau, V., J. Svay-Lucas, L. Nicoletis, and H. Rakotoarisoa, 2000, 3D true-amplitude migration by regularization in angle domain: Presented at the 62nd Annual International Conference and Exhibition, EAGE.

Ursin, B., 2004, Parameter inversion and angle migration in anisotropic elastic media: Geophysics, **69**, 1125–1142.

Wu, R. S., and L. Chen, 2006, Directional illumination analysis using beamlet decomposition and propagation: Geophysics, **71**, S1147–S1159.

Xu, S., H. Chauris, G. Lambaré, and M. Noble, 2001, Common-angle migration: A strategy for imaging complex media: Geophysics, **66**, 1877–1894.